Gait Adaptation after Leg Amputation of Hexapod Walking Robot without Sensory Feedback

Jan Feber[0000−0001−6546−7187], Rudolf Szadkowski[0000−0003−4075−116X], and Jan Faigl[0000−0002−6193−0792]

Department of Computer Science, Faculty of Electrical Engineering
Czech Technical University in Prague
Technická 2, 166 27, Prague 6, Czech Republic
{feberja1,szadkrud,faiglj}@fel.cvut.cz,
WWW home page: https://comrob.fel.cvut.cz/

Abstract. In this paper, we address the adaptation of the locomotion controller to change of the multi-legged walking robot morphology, such as leg amputation. In nature, the animal compensates for the amputation using its neural locomotion controller that we aim to reproduce with the Central Pattern Generator (CPG). The CPG is a rhythm-generating recurrent neural network used in gait controllers for the rhythmical locomotion of walking robots. The locomotion corresponds to the robot's morphology, and therefore, the locomotion rhythm must adapt if the robot's morphology is changed. The leg amputation can be handled by sensory feedback to compensate for the load distribution imbalances. However, the sensory feedback can be disrupted due to unexpected external events causing the leg to be damaged, thus leading to unexpected motion states. Therefore, we propose dynamic rules for learning a new gait rhythm without the sensory feedback input. The method has been experimentally validated on a real hexapod walking robot to demonstrate its usability for gait adaptation after amputation of one or two legs.

Keywords: Gait adaptation · Robot locomotion · Leg amputation · Hexapod walking robot · Damage compensation · Emergent system · Dynamic system · CPG-RBF

1 Introduction

Dealing with damaged limbs is desirable to keep the walking robot operable in a long-term mission. During the mission, various leg malfunctions can occur, such as a leg can get stuck, be crashed by a fall of a heavy object or stop working correctly due to component wear. It might be preferable to amputate (lose) the leg instead of keep using the damaged limb. Hence, we need a mechanism to deal with the locomotion change after the leg amputation.

Adjusting to morphological changes like amputation is essential for living organisms to survive. Existing organisms have voluntary leg amputation included

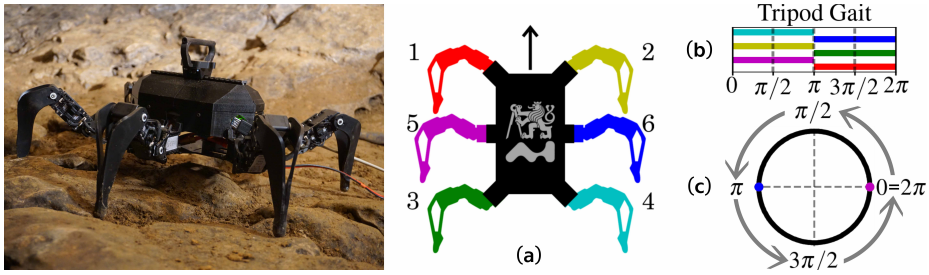

Fig. 1. On the left, a photo of the hexapod walking robot used in experiments is shown. The (a) presents the schema and labeling of the robot's legs. The arrow points in the walking direction. (b) and (c) are different ways of describing the tripod gait pattern, which is used in our experiments as a starting point before the amputation. The colorful bars in (b) correspond to the swing duration within the movement phase ($[0, 2\pi)$ on the horizontal axis). The colors correspond to color labeling from (a). (c) presents the phase as a cycle, as it repeats periodically. The colorful dots represent the start of the corresponding leg's swing (i.e., the value ϕ_i^s). The dots are overlapping because the start of the swing is the same for the legs within the triplets $(1, 3, 6)$ and $(2, 4, 5)$.

as their defense mechanism called autotomy, and some species are even able to regenerate the lost limb after a certain time [5]. Nevertheless, both types of species (with and without the ability to regrow the lost limb) adapt to the morphological change after the amputation. The adaptation mechanisms observed on legged animals are imitated by researchers in developed biomimetic models.

A frequently used biomimetic mechanism is the concept of the *Central Pattern Generator* (CPG), a recurrent neural network producing rhythm underlying the locomotion [8]. The CPG's resistance to perturbations is utilized in CPG-based locomotion controllers [17]. The periodic movement induced by CPGs is called a gait pattern. It is a repetitive motion pattern described by the mapping between the phase of the gait and limb movement timing. The movement of each leg consists of swing (the leg's forward movement) and stance, the backward movement of the leg pushing against the ground, and moving the body forward. The swing and stance repeat periodically, altering each other.

Damage-compensation approaches for hexapod control can be based on sensory feedback such as the WALKNET architecture [2,12,13] or [9,10]. However, the sensory feedback, especially in the case of leg malfunction, may not be reliable. Moreover, the feedback is strongly influenced by the terrain changes, such as feedback on an uneven vs. plane surface or feedback on sand or mud differs from feedback on a pavement. Hence, it is desirable to have an adaptation method that does not rely on explicit sensory feedback.

In this work, we propose dynamic rules to adjust the legs' movement rhythm producing a stable gait pattern with one amputated leg or one amputated leg on each side of the robot's body. The proposed approach is based on the CPG-RBF architecture [11] connecting the CPG with the *Radial Basis Function* (RBF) neurons that encode the mapping between the CPG's phase and the robot's

motion. As the centers of RBF neurons are placed along the CPG's cyclic attractor, the RBF neurons are activated periodically producing the rhythm for locomotion. In the previous work, we proposed a method for mapping the RBF neurons on the limit cycle ordered correctly to produce a rhythm for a given gait pattern [4]. In the present work, we extend the method to enable gait adaptation to the amputation of one or two legs. We propose self-organizing dynamics that adapt to changed morphology caused by an amputation with respect to *Inter-Leg Coordination Rules* (ICRs) [2], where the RBF centers are shifted around the limit cycle to avoid the ICR violation. We demonstrate the usability of the proposed method by its deployment on a real hexapod walking robot and experimental validation in four different scenarios with one and two amputated legs.

2 Related Work

Various architectures used in CPG-based controllers can be found in the literature. Architectures with one or more uncoupled CPGs for each leg have been proposed [9,10]. On the contrary, architectures with inter-coupled CPGs and synchronized by sensory input can be found [14,7,16]. Besides, the controllers can consist of two sub-modules: amplitude control, providing the magnitude of actuation, and phase control, providing the actuation in which the CPG is involved. Hence, we can further distinguish approaches based on the phase control mapping between the movement and the CPG's phase.

The mapping can be a continuous, binary-phase switch or the generalization of the latter, a multi-phase switch. Continuous mapping transforms the CPG signal directly into the motion commands by reshaping the waveform with different continuous functions [16,15]. As the motion commands are tightly coupled to the waveform, any change of the CPG-generated waveform requires finding a new continuous function providing the appropriate commands, which is generally a complex problem. On the other hand, the dependency between the waveform and commands is relaxed in the binary-switch mapping that uses the CPG as a timing switch between the stance and swing phases, with each of the phases having its control rules [6].

In this paper, we follow the multi-phase switch represented by the CPG-RBF architecture [11,14]. We propose to take advantage of the multi-phase methods compared to the continuous mapping, which is the independence of the CPG model. In contrast to the binary-switch, the multi-phase model enables more control over the motion because we gain more information about the ongoing gait phase than switching only between swing and stance modes.

Existing architectures dealing with leg malfunctions include WALKNET [2] further developed in [12,13]. There are methods relying on the sensory feedback as a coupling mechanism for the CPGs that are not interconnected directly but interact indirectly through the sensory feedback from the environment [9]. A principle of tegotae incorporating the sensory feedback to influence the CPGs phase by detecting unwanted gait behavior is introduced in [10]. However, we

assume the sensory feedback might be unreliable after body and leg damage in the proposed approach. Therefore, we propose an adaptation of the locomotion to the morphology change only with respect to (w.r.t) the coordination rules. The proposed method is an extension of the parametrizable gait generator based on the CPG-RBF architecture [4] that reacts to the leg amputation by adjusting the RBF neurons w.r.t. the inter-leg coordination rules.

3 Problem Specification

The gait phase controller drives the leg movement rhythm that controls the swing and stance timing. The controller should follow the *Inter-leg Coordination Rules* (ICRs) observed from gaits of hexapod insects [2] to ensure stability. Three rules can be defined as follows.

1. While a leg is lifted-off, suppress the lift-off of the consecutive leg.
2. If the leg touches the ground, initiate the lift-off of the consecutive leg.
3. Do not lift off the contralateral legs at the same time.

Following the ICRs, the exact gait pattern is given by the phase offset $\Delta\phi$ of the consecutive legs motion phase (e.g., for the tripod gait $\Delta\phi = \pi$) that corresponds to the swing phase duration [1].

The ICRs, in combination with gait-determining $\Delta\phi$, work well for regular gait patterns; however, the conditions change with the leg amputation. For instance, the amputated leg behaves like in the swing phase, (i.e., being lifted-off of the ground) and its contralateral and consecutive leg can never undergo the swing movement, based on the ICRs. The relations between the legs have to be adjusted to keep the controller functional after the amputation.

With lowering the number of legs, we also need to consider the number of legs supporting the robot's body, i.e., the legs in the stance phase. An example is using the tripod gait (leg triplets $1, 3, 6$ and $2, 4, 5$ altering in the swing phase longing for half of the period, see Fig. 1) with no adjustment after the amputation of the leg 6. It results in both remaining legs from the right side of the robot's body being lifted simultaneously; therefore, the robot has no support on the right side and falls. The original gait patterns have to be modified in the case of the amputation to prevent the robot's body from falling to the ground.

The swing duration $\Delta\phi$, corresponding to the phase offset of consecutive legs' movement, can also conflict with the ICRs after the amputation. Let us consider the tripod gait with the amputation of the leg 6. The legs 2 and 4 have to alter each other to keep at least one leg from the body's right side on the ground to support the robot's body and keep the swing phase length equal to $\Delta\phi = \pi$. It means that their respective contralateral legs can not undergo the swing simultaneously, according to the third ICR. Hence, one of the legs 1 or 3 has to undergo the swing simultaneously with the leg 5, which is, however, in contradiction with the first ICR. The swing duration $\Delta\phi$, corresponding to the minimal phase offset of consecutive legs, has to be modified in some cases to maintain the gait stable according to ICRs.

The gait rhythm is given by the phases in which the legs undergo swing and stance movement. The beginning and end of the swing (the swing end is the start of the stance) are given by the activation phase $\phi_i^s \in [0, 2\pi)$ and $\phi_i^e \in [0, 2\pi)$, respectively.

In our previous work [4], we introduced a mechanism for mapping the RBF centers positions within the CPG's phase space based on the phase activation values. Hence, the problem of moving the RBF centers within the CPG's phase space simplifies to shifting the activation phases ϕ_i^s and ϕ_i^e within the interval $[0, 2\pi)$. In this paper, we propose dynamic rules depending on the ICRs, swing duration $\Delta\phi$ and knowledge about limb amputation. The proposed dynamics update $\Delta\phi$ and the swing start and end phases ϕ_i^s and ϕ_i^e are shifted for each functioning leg i to achieve a stable gait pattern compliant with ICR.

4 Proposed Locomotion Adaptation to Leg Amputation

We propose update rules for swing duration $\Delta\phi$ and start phase ϕ_i^{s} that continually minimize the motion errors inferred from the: (i) detected ICRs violations; and (ii) over-safe states. At any time t, the ICRs determine whether the i-th leg should be in stance, $d_i(t) = 1$, w.r.t. other legs motion $s_j^{\mathrm{sw}}(t)$ and damage $s_j^{\mathrm{dmg}}(t)$ states; where $s_j^{\mathrm{sw}} = 1$ denotes the j-th leg in the swing, while $s_j^{\mathrm{dmg}} = 1$ denotes the j-th leg being amputated. The motion states $\mathbf{s}^{\mathrm{sw}}$ determine whether the robot is in an over-safe state. The proposed system adjusts the swing duration, and minimizes the duration of the over-safe state and ICRs violation; thus, the swing phases ϕ_i^{s} converge to a gait configuration allowing the hexapod robot to walk again.

4.1 Morphology Information

The restrictions given by the ICRs based on the robot's morphology do not provide clear guides for the leg relations after a significant morphology change, like an amputation. In the original work [2], where the ICRs were proposed, are rules related to the load distribution among the legs. However, the rules require non-trivial sensory feedback, which does not have to be available nor undistorted. Hence, we propose to add the following four rules to the ICRs that complement the originally introduced ICRs [2], altering the consecutivity and contralaterality within the legs after the leg amputation. The proposed *Consecutivity and Contralaterality Adjustment Rules* (CCARs) are as follows.

1. The most-front left (right) functional leg is a contralateral leg for the most-front right (left) functional leg.
2. The most-hind left (right) functional leg is a contralateral leg for the most-hind right (left) functional leg.
3. If the leg i is contralateral leg of the leg j that becomes contralateral leg for the leg k due to the proposed rule 1. or 2., then the contralateral relation between the legs i and j is no longer active.

4. If the leg j: (i) has consecutive leg k, and (ii) is the i-th leg's consecutive leg, and (iii) is not functional, then the leg k becomes the consecutive leg of the leg i.

The application of the CCARs enables us to use the ICRs even for a robot with amputated legs. An example of the relations after the amputation is visualized in Fig. 2.

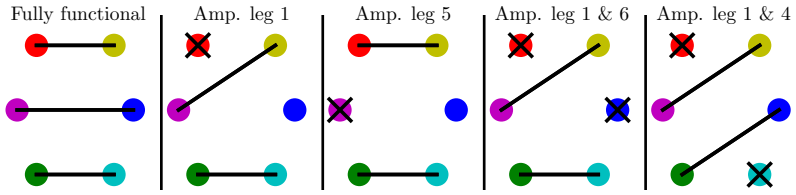

Fig. 2. The schema presents scenarios of the amputation in our experiments and the application of the CCARs 1., 2. and 3., where contralateral relation is depicted by the edge between respective legs' nodes. A cross over the node represents amputation. The colors of the legs' nodes correspond to the leg labeling in Fig. 1

4.2 Gait Swing Control

The gait is determined by the swing starts ϕ_i^{s} and the swing duration $\Delta\phi$ that parameterize the control signal generated by the employed CPG-RBF architecture

$$\dot{y} = \omega + \alpha(t)\sin(y), \tag{1}$$

$$\varphi(t;\phi) = \exp(-\lambda(y(t) - \phi)^2), \tag{2}$$

where ω is the CPG frequency and the hyperparameter λ determines the width of the bell-shaped RBF signal. The model (1) is a simplified CPG model, where the perturbation $\alpha(t)$ is considered to be zero during the locomotion learning. The i-th leg swing start is driven by the RBF signal $\varphi_i^{\mathrm{s}}(t) = \varphi(t;\phi_i^{\mathrm{s}})$ and the end with $\varphi_i^{\mathrm{e}}(t) = \varphi(t;\phi_i^{\mathrm{s}} + \Delta\phi)$. The peaks of the signals $\varphi_i^{\mathrm{s}}(t)$ and $\varphi_i^{\mathrm{e}}(t)$ switch the motion state $s_i^{\mathrm{sw}}(t)$ to one and zero, respectively.

4.3 ICRs Violation Detection

The swing control should be configured so that it minimizes the duration of the possible ICRs violations and over-safe state. The violation of the ICRs can be inferred from the motion $\mathbf{s}^{\mathrm{sw}}(t)$ and amputation $\mathbf{s}^{\mathrm{dmg}}(t)$ states using propositional logic as follows.

Let $f : (\mathbf{s}^{\mathrm{sw}}, \mathbf{s}^{\mathrm{dmg}}) \to \mathbf{d}$ represent the ICRs as a boolean function that maps the legs swing and damage to required stances $\mathbf{d} \in \{0,1\}^6$, where $d_i = 1$ represents the i-th leg is required to be in stance and thus not lose the balance. Therefore, if the leg is required to be in the stance but is in the swing, $d_i(t) \wedge s_i^{\mathrm{sw}}(t)$, we can detect the rule violation. We distinguish the rule violation at the start and end of the swing

$$a_i^{\mathrm{s}}(t) = d_i(t) s_i^{\mathrm{sw}}(t) [\![\varphi_i^{\mathrm{s}} > \delta]\!], \tag{3}$$

$$a_i^{\mathrm{e}}(t) = d_i(t) s_i^{\mathrm{sw}}(t) [\![\varphi_i^{\mathrm{e}} > \delta]\!], \tag{4}$$

respectively, where $\delta = 0.95$ is the hyperparameter thresholding the RBF neuron signal peak. The violation signals a_i^{s} and a_i^{e} are then smoothed by integration

$$\dot{v}_i^{\mathrm{s/e}} = \begin{cases} 1 - v_i^{\mathrm{s/e}} \text{ if } a_i^{\mathrm{s/e}} = 1, \\ -v_i^{\mathrm{s/e}} \text{ if } a_i^{\mathrm{s/e}} = 0, \end{cases} \tag{5}$$

outputting the error signals for the start v_i^{s} and end v_i^{e} of the i-th leg swing.

4.4 Phase Action Values Ordering

The swing start ϕ_i^{s} minimizes the duration of ICRs violation by the following update rule w.r.t. the motion error signals

$$\dot{\phi}_i^{\mathrm{s}} = v_i^{\mathrm{s}} - v_i^{\mathrm{e}} + \mathrm{sgn}(\phi_i^{\mathrm{s}} - \phi_j^{\mathrm{s}} + \pi)(\phi_i^{\mathrm{s}} - \phi_j^{\mathrm{s}} + \pi)^2, \tag{6}$$

where the first two terms push the swing start outside the time interval during which the i-th leg should be in the stance, the third term is a regularization pushing the i-th leg into the antiphase to its contralateral j-th leg, and the function $\mathrm{sgn}(x)$ is the sign function.

4.5 Swing Duration Adjustment

The long-term ICRs violation $v(t) = \sum_i v_i^{\mathrm{s}}$ or over-safe state $o(t) = \prod_i (1 - s_i^{\mathrm{sw}}(t))$ (when all legs are in the stance at the same time) require a change in the swing duration. We propose to detect the long-term error states with two *Leaky-Integrate&Fire* (LIF) neurons $c_o(t)$ and $c_v(t)$. The LIFs $c_o(t)$ and $c_v(t)$ integrate their respective inputs $o(t)$ and $v(t)$ and it fires if the LIF state surpasses the threshold. The LIF firing indicates the long-term error state, which is then addressed by the swing duration update rule

$$\dot{\Delta\phi} = \begin{cases} \xi & \text{if } c_o \text{ fires}, \\ -\xi & \text{if } c_v \text{ fires}, \\ 0 & \text{otherwise} \end{cases} \tag{7}$$

where $\xi = 0.2$ is the speed of $\Delta\phi$ decrease and increase.

The update rules for the swing duration $\Delta\phi$ and swing phase ϕ_i^{s} miniminze the motion error duration continually. The feasibility of the proposed approach has been experimentally verified on real hexapod walking robots; the results are reported in the following section.

5 Experimental Results

The feasibility of the proposed solution has been evaluated on four amputation scenarios deployed on a real hexapod walking robot. All the presented scenarios start with the robot walking using a pre-trained tripod gait, which is interrupted by amputation after five hundred iterations (approximately two complete gait cycles). The scenarios are depicted in Fig. 2, where two of them show the adapting process after the amputation of one leg (the legs 1 and 5), and the other two show the amputation of two legs denoted 1&6, and 1&4. Each of the four scenarios was run ten times, where the proposed algorithm converges to a stable solution as indicated in Fig. 3. Since the ICRs violation indicator v_i^s, inducing the rhythm change, approaches zero, the gait pattern is compliant to the ICRs adjusted by the proposed CCARs.

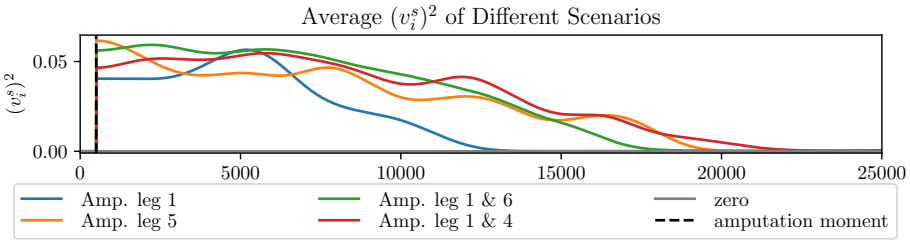

Fig. 3. The average of the value $(v_i^s)^2$ with increasing iteration number during the performed amputation scenarios depicted in Fig. 2 computed from ten experimental trials performed. Each color represents the average value of $(v_i^s)^2$ for each leg from all experiments of the particular scenario. Blue and orange curves show the one leg amputation scenarios for the leg 1 and 5, respectively. The two legs amputation scenarios for the pairs 1&6 and 1&4 are depicted in green and red, respectively. The dashed black line represents the moment of the amputation. The standard deviations in the last state are $5 \cdot 10^{-17}, 4 \cdot 10^{-6}, 4 \cdot 10^{-6}$ and $3 \cdot 10^{-6}$ for the scenarios represented by blue, orange, green, and red lines, respectively.

Examples of the resulting gait patterns are visualized in Fig. 4, where the upper plots show the gait schema right after the amputation and the lower plots present the adjusted gait rhythm. Note the adjustment of the swing length and the difference in the amount of conflicting areas between one and two amputated legs scenarios.

The update rule for the swing duration $\Delta\phi$ and the activity of the LIF neurons is demonstrated in Fig. 5.

The four experiments were realized with deployment on the real hexapod walking robot [3] depicted in Fig. 1. The robot has six legs, each with three joints made of the Dynamixel AX-12 servomotors. The body motion is achieved by the open-loop controller setting the joint angles resulting in a swing and stance motion. The swing of each i-th leg is parameterized by the swing start ϕ_i^s

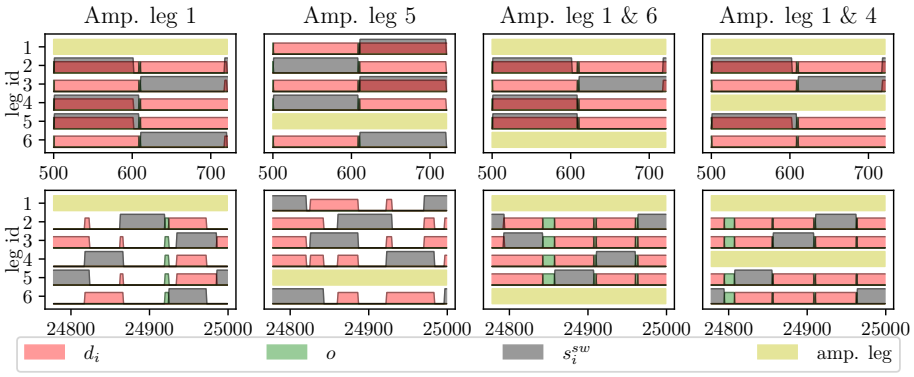

Fig. 4. Visualization of approximately one gait period of the leg rhythm for performed amputation scenarios introduced in Fig. 2. The upper plots show the state right after the amputation, which occurred in the 500-th iteration. The lower plots show adjusted rhythm after the converged learning. Each row of the sub-figure represents one leg (given by the leg's number on the vertical axis). The yellow bar indicates the amputated leg; the grey bar represents the swing phase of the motion; the red bar represents the state when $d_i = 1$ for the i-th leg; and the green bar represents the over-safe state $o = 1$.

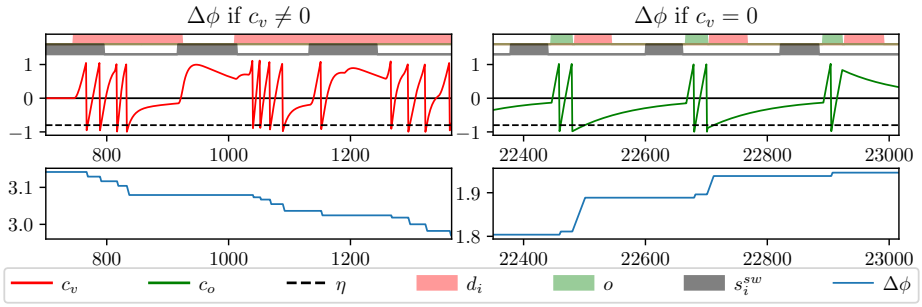

Fig. 5. Visualization of the LIF mechanism (red and green curves in the upper plots) and its influence on the swing duration $\Delta\phi$ (blue curve in the lower plots). The left LIF is inhibited by the violation of the ICRs and CCARs indicated by bars above the plot, where the grey bar represents the swing phase, and the red bar represents the area in which the performance of the swing action would violate the rules. Note, that the LIF (red line) is depdendent on v_i of all legs while the shown grey and red bars represents only one leg's swing and rules violation indicator. Once the LIF integrates into one, it fires and decreases its value below the threshold indicated by the dashed black line. The value below the threshold induces lowering $\Delta\phi$ in the lower plot. The same mechanism is applied in the right plot, where the inhibition is provided by the over-safe state o (shown by the green bar in the schema above the plot) if no violation is detected. However, here hitting the threshold implies the growth of $\Delta\phi$.

and end ϕ_i^{e} phases, given by the proposed phase controller, and by two additional phases ϕ_i^{m} and ϕ_i^{cm} placed in phase between ϕ_i^{s} and ϕ_i^{e} (i.e., middle of the swing) and between ϕ_i^{e} and ϕ_i^{s} (i.e., middle of the stance), respectively.

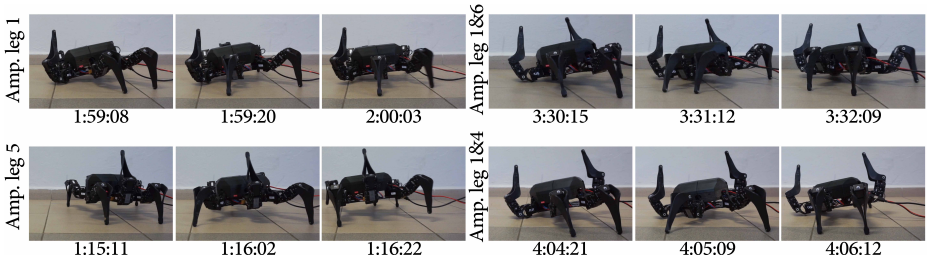

Fig. 6. Snapshots of the resulting gaits for all four performed experimental scenarios. The amputation was simulated by lifting the amputated leg above the robot's body so as not to touch the ground. The robot walks from right to left. The numbers below the photos represent the experiment time in the format *minutes:seconds*. The length of the learning process is influenced by the impact of the amputated leg absence on the gait stability. In general, the loss of the the most-front (most-hind) leg is worse for the stability than the loss of the middle leg, because the most-front (most-hind) leg prevents the body from falling forward (backward), while the middle leg *"only"* improves the overall balance. Hence, the new gait rhythm learning process was longer for experiments with amputated front or hind legs (i.e., scenarios Amp. leg 1 and Amp. leg 1&4) than for experiments with the middle leg amputated (i.e., Amp. leg 5 and Amp. leg 1&6).

In the experimental setup, the robot walked forward for two gait cycles of the tripod gait on an office floor. Then, the amputation was simulated by permanently lifting the corresponding legs so they do not touch the ground in any gait phase. The robot reacts to the amputation by organizing the gait pattern into a pattern compliant with the ICRs and producing a new gait that enables the robot to continue its forward motion. The experimental performance is captured in Fig. 6 and video supplementary materials.

We can conclude that the proposed method converges to a stable solution in all reported experimental scenarios. The stable solution is a new gait pattern adjusted to the morphological changes caused by leg amputation.

6 Conclusion

We proposed and experimentally verified self-organizing dynamics for changing the gait rhythm after leg amputation on a hexapod walking robot. The method builds on the CPG-RBF-based controllers, and we propose an alternative and complementary solution for damage-control for architectures based purely on sensory feedback. The proposed method detects the violation of the *Inter-leg Coordination Rules* extended by the proposed *Consecutivity and Contralaterality*

Adjustment Rules. The detections is then used to adjust the rhythm to avoid the violation in the following gait cycles. The rhythm change itself is not always enough to avoid the rules violation. Hence, the proposed mechanism introduces the dynamic change of the swing phase duration to support resolving the conflict. In combination, the swing phase duration change and the shift of the swing in the phase produce a new gait rhythm after the amputation.

The feasibility of the method is demonstrated by its deployment on the real hexapod walking robot in four various amputation scenarios. However, it is intended to be used with sensory-based amputation compensation methods. In the case of sensory-feedback failure, the proposed method would compensate for the gait control. Two shortcomings can be addressed in future work. The method needs further adjustments to be applicable for robots with different morphology than hexapods. Besides, the proposed method does not resolve the loss of two or more limbs on the same side of the robot's body by using the introduced rules.

Acknowledgments – This work has been supported by the Czech Science Foundation (GAČR) under research project No. 21-33041J.

References

1. Chen, W., Ren, G., Zhang, J., Wang, J.: Smooth transition between different gaits of a hexapod robot via a central pattern generators algorithm. Journal of Intelligent & Robotic Systems **67**(3), 255–270 (2012)
2. Dürr, V., Schmitz, J., Cruse, H.: Behaviour-based modelling of hexapod locomotion: linking biology and technical application. Arthropod Structure & Development **33**(3), 237–250 (2004), arthropod Locomotion Systems: from Biological Materials and Systems to Robotics
3. Faigl, J., Čížek, P.: Adaptive locomotion control of hexapod walking robot for traversing rough terrains with position feedback only. Robotics and Autonomous Systems **116**, 136–147 (2019). https://doi.org/10.1016/j.robot.2019.03.008, https://doi.org/10.1016/j.robot.2019.03.008
4. Feber, J., Szadkowski, R., Faigl, J.: Gait genesis through emergent ordering of rbf neurons on central pattern generator for hexapod walking robot. In: Conference Information Technologies - Applications and Theory (ITAT). pp. 114–122 (2021)
5. Fleming, P.A., Muller, D., Bateman, P.W.: Leave it all behind: a taxonomic perspective of autotomy in invertebrates. Biological Reviews **82**(3), 481–510 (2007). https://doi.org/https://doi.org/10.1111/j.1469-185X.2007.00020.x, https://onlinelibrary.wiley.com/doi/abs/10.1111/j.1469-185X.2007.00020.x
6. Fukuoka, Y., Kimura, H., Hada, Y., Takase, K.: Adaptive dynamic walking of a quadruped robot 'tekken' on irregular terrain using a neural system model. In: 2003 IEEE International Conference on Robotics and Automation (Cat. No.03CH37422). vol. 2, pp. 2037–2042 vol.2 (2003). https://doi.org/10.1109/ROBOT.2003.1241893
7. Gay, S., Santos-Victor, J., Ijspeert, A.: Learning robot gait stability using neural networks as sensory feedback function for central pattern generators. In: 2013 IEEE/RSJ International Conference on Intelligent Robots and Systems. pp. 194–201 (2013). https://doi.org/10.1109/IROS.2013.6696353

8. Mantziaris, C., Bockemühl, T., Büschges, A.: Central pattern generating networks in insect locomotion. Developmental Neurobiology **80**(1-2), 16–30 (2020). https://doi.org/https://doi.org/10.1002/dneu.22738, https://onlinelibrary.wiley.com/doi/abs/10.1002/dneu.22738
9. Miguel-Blanco, A., Manoonpong, P.: General distributed neural control and sensory adaptation for self-organized locomotion and fast adaptation to damage of walking robots. Frontiers in Neural Circuits **14** (2020). https://doi.org/10.3389/fncir.2020.00046, https://www.frontiersin.org/article/10.3389/fncir.2020.00046
10. Owaki, D., Goda, M., Miyazawa, S., Ishiguro, A.: A minimal model describing hexapedal interlimb coordination: The tegotae-based approach. Frontiers in Neurorobotics **11** (2017). https://doi.org/10.3389/fnbot.2017.00029, https://www.frontiersin.org/article/10.3389/fnbot.2017.00029
11. Pitchai, M., Xiong, X., Thor, M., Billeschou, P., Mailänder, P.L., Leung, B., Kulvicius, T., Manoonpong, P.: Cpg driven rbf network control with reinforcement learning for gait optimization of a dung beetle-like robot. In: Tetko, I.V., Kůrková, V., Karpov, P., Theis, F. (eds.) Artificial Neural Networks and Machine Learning – ICANN 2019: Theoretical Neural Computation. pp. 698–710. Springer International Publishing, Cham (2019)
12. Schilling, M., Cruse, H., Arena, P.: Hexapod walking: an expansion to walknet dealing with leg amputations and force oscillations. Biological Cybernetics **96**(3), 323–340 (Mar 2007). https://doi.org/10.1007/s00422-006-0117-1, https://doi.org/10.1007/s00422-006-0117-1
13. Schneider, A., Paskarbeit, J., Schaeffersmann, M., Schmitz, J.: Hector, a new hexapod robot platform with increased mobility - control approach, design and communication. In: Rückert, U., Joaquin, S., Felix, W. (eds.) Advances in Autonomous Mini Robots. pp. 249–264. Springer Berlin Heidelberg, Berlin, Heidelberg (2012)
14. Szadkowski, R., Faigl, J.: Neurodynamic sensory-motor phase binding for multi-legged walking robots. In: International Joint Conference on Neural Networks (IJCNN). pp. 1–8 (2020)
15. Thor, M., Manoonpong, P.: A fast online frequency adaptation mechanism for cpg-based robot motion control. IEEE Robotics and Automation Letters **4**(4), 3324–3331 (2019). https://doi.org/10.1109/LRA.2019.2926660
16. Yu, H., Gao, H., Ding, L., Li, M., Deng, Z., Liu, G.: Gait generation with smooth transition using cpg-based locomotion control for hexapod walking robot. IEEE Transactions on Industrial Electronics **63**(9), 5488–5500 (2016). https://doi.org/10.1109/TIE.2016.2569489
17. Yu, J., Tan, M., Chen, J., Zhang, J.: A survey on cpg-inspired control models and system implementation. IEEE Transactions on Neural Networks and Learning Systems **25**(3), 441–456 (2014)